Composition dependence of Ag photodoping into amorphous Ge-S films

Takeshi Kawaguchi and Shigeo Maruno
Department of Electrical and Computer Engineering, Nagoya Institute of Technology, Showa-ku, Nagoya 466, Japan

(Received 7 August 1991; accepted for publication 18 November 1991)

Photodoping kinetic studies of thin sample of Ag/Ge_xS_{100-x} ($21<x<45$) were made through optical transmission measurements. The initial photodoping rate increases with increasing S content, whereas the total amount of dissolved Ag shows a maximum around the stoichiometric composition GeS_2. The results are similar to those of the Ag/Ge-Se system but different from the Ag/As-S system. The composition dependencies are qualitatively explained by the structure of Ge-S bulk glass and the glass-forming ability of Ag-Ge-S bulk glass. In this study it was also found that aging effect is considerable within several hours after sample preparation and a reciprocity law holds between the initial rate and illumination power.

I. INTRODUCTION

Photodoping of metals such as Ag into amorphous chalcogenide semiconductors has been extensively studied by many workers, because of fundamental and technological interests. Although the various experimental data have been reported, no consensus has been reached concerning the interpretation of the phenomenon. A systematic study of composition dependence for the chalcogenide layer is important to make the mechanism clear and to search for the most suitable material for the applications to high-contrast optical recording device and high-resolution microlithography. Recently, the ultrahigh resolution ($\sim$500-Å width) was obtained with the Ge-based chalcogenide using a soft x ray of synchrotron radiation.[1]

For the As-based chalcogenides, a significant advance is seen on the mechanism and the explanations of several characteristic features such as a steplike diffusion profile of Ag.[2,3] A similar idea seems to be applied to the Ge-based system. Recently, Calas, Ghrandi, and Galibert[4] and Kluge *et al.*[5] reported the photodoping kinetics of the Ag/Ge-Se system. Several points are different from the composition dependence of the Ag/As-S system, such as the initial photodoping rate and total amount of photodoped Ag. Thus, it is of interest whether the kinetics of the Ag/Ge-S system is similar to the Ag/Ge-Se or Ag/As-S systems. Several reports have been published for the samples of composition around GeS_2.[6–9] However, a systematic study for the Ag/Ge-S system has not been performed, though this system is a candidate as a high-resolution lithographic resist being sensitive to uv light. Moreover, it has advantages of being nontoxic and thermally stable.[9]

Since the Ge-S film is widely different from the As-S film with regard to the film structure, the difference seems to influence the photodoping process, especially at the early stage, such as the initial photodoping rate (induction period). On the other hand, properties such as the total amount of photodissolved Ag (Ag concentration in the doped region) seem to be associated with the amorphous forming ability (thermodynamic stability of Ag-containing amorphous phase). Thus, the composition dependence is quantitatively expressed in the initial rate and the total amount of doped Ag.

In this study, several fundamental properties were also found using an $Ag/Ge_{30}S_{70}$ sample: (i) The initial photodoping rate increases considerably by the aging effect at room temperature; (ii) structural relaxation by the aging effect is remarkable for the Ag layer rather than the $Ge_{30}S_{70}$ layer; and (iii) the reciprocity law holds between the initial photodoping rate and the illumination power.

II. EXPERIMENTS

A. Sample preparation and exposure

The Ge_xS_{100-x} glass or crystalline ingots ($x = 20$, 25, 30, 33, 35, 40, 45, and 50) were prepared by quenching in water after melting and stirring a mixture of the constituent elements (Ge: 99.999%; S: 99.999%) at 1000 °C for 10 h in evacuated silica ampoules. The fragments of crushed ingot were evaporated onto a cleaned glass substrate from a W basket in a vacuum of $\sim 10^{-6}$ Torr. The compositions of the amorphous films were analyzed by electron-probe microanalyzer (EPMA) (JEOL, JCXA-733) with energy-dispersive x-ray (EDX) facility (Tracor Northern, TN-5500) using crystals of Ge and α-GeS_2 as the standard materials. The films of $x = 21$, 24.5, 30, 34, 35, 38, 42, and 45 were obtained by evaporating the raw ingots of $x = 20$, 25, 30, 33, 35, 40, 45, and 50, respectively, indicating that the compositions of the films except $x<35$ deviate from those of the raw ingots by evaporation. Silver (99.99%) was evaporated onto the Ge-S films in a vacuum of $\sim 10^{-6}$ Torr without breaking vacuum between the evaporations.

The respective deposition rates were monitored with a quartz oscillator (Ge-S: 3–5 Å/s; Ag: 10–15 Å/s). The thicknesses of the films were checked using a mechanical stylus instrument (Sloan, Dektak II) or by optical transmission measurements. The temperature of the glass substrate was maintained at 20 ± 2 °C. The Ag-Ge-S phase is presumably formed on the Ge-S layer at an early stage of the Ag deposition. Since the composition of the phase is

 0021-8979/92/052195-07$04.00

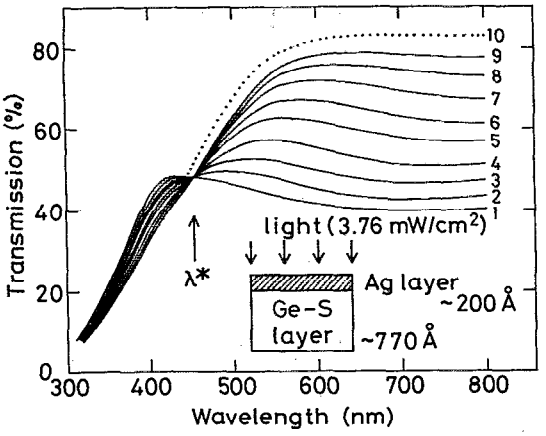

FIG. 1. Change in optical transmission spectra resulting from Ag photodoping into amorphous $Ge_{24.5}S_{75.5}$ film. The curves numbered 1–10 correspond to the spectra after exposure to light for 0, 4, 11, 22, 37, 55, 76, 99, 124, and 410 min, respectively. An arrow at 452 nm in wavelength indicates the isotransmission point λ^*. The spectrum at the final stage of photodoping (dotted line) deviates from λ^*.

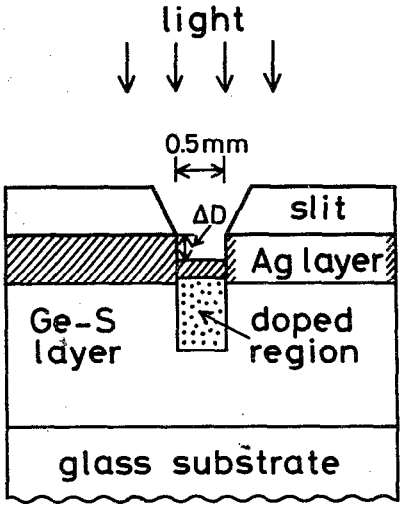

FIG. 2. Scheme of decrease in sample thickness by photodoping. Depth of the photodoped region, ΔD was determined through stylus measurement and checked by SEM observation. A slit was put on the sample as a mask during exposure.

unknown, the photodoping sample is named as Ag/Ge_xS_{100-x} in this paper without the Ag-Ge-S phase.

The photodoping samples were irradiated with the light of an ultrahigh-pressure Hg lamp (Ushio, 500D) through two lenses and an ir-cut filter. The irradiation was done from the Ag-layer side. The change in the optical transmission spectra of the photodoping sample as measured using a double-beam spectrophotometer (Shimadzu, UV-200S). The photodoping experiments were done in air at 20 ± 2 °C.

B. Evaluation of the amount of photodoped Ag

Although the amount of photodoped Ag has been evaluated by various methods (e.g., electrical resistance of the Ag layer,[10,11] x-ray reflection intensity of the Ag layer,[2,12,13] optical reflectivity of the chalcogenide layer,[14,15] chemical etching of the Ag-doped layer,[16,17] and Rutherford backscattering spectrometry[5,18,19]), in this study we evaluated it through the measurements of the optical transmission spectra of the photodoping sample. The thin samples (Ge-S: 500–770 Å; Ag: 200–260 Å) were used in the experiment to avoid the interference effect in the transmission spectra.[6] The thin sample is also suitable for optical memory devices and inorganic resists with ultrahigh resolution.[1]

As an example, the change in the transmission spectra of the thin $Ag/Ge_{24.5}S_{75.5}$ sample by photodoping is shown in Fig. 1. There is an isotransmission point λ^* at 452 nm in wavelength where the transmission is practically independent of the irradiation time. The appearance of λ^* in the spectra satisfies the following important conditions:[6] (i) The dissolved Ag distributes uniformly in the doped region (steplike profile); and (ii) the spectra are not modulated by the interference effect. The λ^* was clearly observed for all the samples of Ag/Ge_xS_{100-x}. As expected in the previous paper,[6] it was found that λ^* shifts toward a longer wavelength with increasing Ge content (e.g., $x=24.5$ at 450 ± 10 nm, $x=30$ at 470 ± 10 nm, and $x=38$ at 500 ± 10 nm).

If λ^* is observed in the transmission data, the amount of photodoped Ag can be estimated from the change in the transmission at any wavelength except λ^* as

$$\ln[T(t)/T(0)] = ky, \tag{1}$$

where $T(t)$ is the transmission of the sample irradiated for time t and y is the amount of dissolved Ag expressed in units of the Ag film thickness.[6] The parameter k concerning the optical density is given by

$$k = \alpha_A - c\alpha_D + (c+d-1)\alpha_{GS}, \tag{2}$$

where α_A, α_D, and α_{GS} are the absorption coefficients of the Ag layer, doped region, and Ge-S layer, respectively. The constants c and d are the structural parameters of the photodoping sample concerning the thickness of the doped region (cy thick) and the decrease in the sample thickness (dy thick), respectively.[6] If k is known, the y value can be determined from the transmission change, $T(t)/T(0)$, at any wavelength except λ^* [Eq. (1)]. In this study, the $T(t)/T(0)$ value was evaluated at 800 nm, since it is usually the greatest in the wavelength range of 300–800 nm.

First, the d value in Eq. (2) for the Ag/Ge_xS_{100-x} samples was determined to know the k value. The thick samples with the Ag layer with various thicknesses (Ge-S: ~5000 Å; Ag: 200–500 Å) were prepared and the d values of the respective samples were determined according to the procedure reported previously.[6]

Then, the decrease in thickness ΔD of the thin samples was examined using the stylus instrument before the saturation of photodoping (Fig. 2). ΔD is expressed as $\Delta D = y + dy$. Thus, y can be obtained from the ΔD and d values as $y = \Delta D/(1+d)$. Finally, the k value can be obtained from $T(t)/T(0)$ and the y value [Eq. (1)]. Since the ΔD values

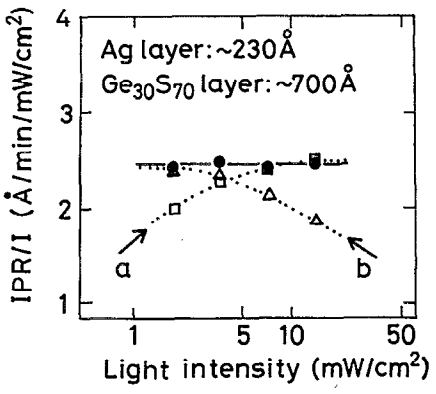

FIG. 3. Relation between initial photodoping rate (IPR) and light intensity I: (□,△) the relation examined immediately after sample preparation; (●) 20 h after the preparation. These data were obtained using a $Ag/Ge_{30}S_{70}$ sample. The ordinate is expressed as IPR/I corresponding to the amount of dissolved Ag per incident total energy at an early stage of photodoping. Two arrows indicate the data obtained (a) from weak light to strong light, and (b) from strong to weak. The solid circles satisfy the reciprocity law between IPR and I.

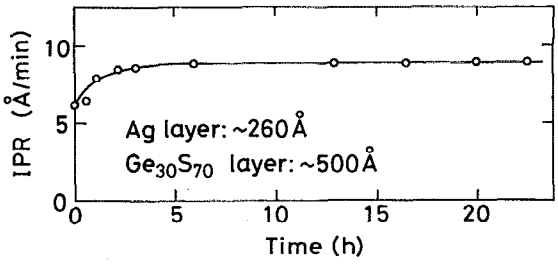

FIG. 4. Change in initial photodoping rate (IPR) by aging effect. The data were obtained using a $Ag/Ge_{30}S_{70}$ sample aged in air (1 atm) at 16±2 °C in the dark. The intensity of the irradiated light was 3.76 mW/cm².

are usually less than 200 Å for the thin sample, the stylus measurement was repeated 5–10 times and the obtained ΔD value was checked by scanning electron microscope (SEM) observation.

Once the k value is determined, the photodoping kinetics (time course of y) is easily obtained by the measurements of transmission of the sample irradiated for various times.

III. RESULTS

A. Reciprocity law concerning illumination power

The photodoping rate can be normalized by the intensity of the irradiated light, if the reciprocity law holds between the doping rate and the light intensity. Therefore, the law for the Ag/Ge-S system was first examined using a $Ag/Ge_{30}S_{70}$ sample. A sample of 2.7×5 cm² was divided into 15 pieces for the experiments at light intensities of 1.9, 3.8, 7.5, and 15 mW/cm².

Figure 3 shows the obtained results between the initial photodoping rate (IPR) and the light intensity I. The IPR was evaluated as the slope of $y(t)$ at the initial stage of photodoping (see the inset of Fig. 5). The IPR for the total incident energy E is defined as dy/dE. It is also expressed as $dy/dE = (dy/dt)/I = \mathrm{IPR}/I$ by the use of the relation $E = It$. Immediately after the sample preparation, the photodoping experiments were carried out from weak light to strong light (□) and from strong to weak (△), as shown by two arrows [(a) and (b) in Fig. 3]. The data do not show a relation of the reciprocity law (if the law holds, the data points lie in parallel with the axis of abscissa). The strange results suggest that the photodoping sample exhibits a remarkable aging effect within the relatively short period.

Then, the aging effect on IPR was examined using the $Ag/Ge_{30}S_{70}$ sample. The samples were aged in air (1 atm) at 16±2 °C under dark. As shown in Fig. 4, IPR increases considerably by the aging effect within 5 h after the sample preparation. The change in the transmission spectra itself by the aging effect was also found over the wavelength range of 300–800 nm (discussed in Sec. IV A). The reciprocity law, therefore, was reexamined using the sample aged for 20 h from the preparation. The obtained IPR/I data were independent of I as shown by solid circles in Fig. 3, indicating that the reciprocity law between IPR and I holds in the photodoping phenomenon. Except for IPR, however, a clear reciprocity law was not observed in the overall range of the kinetics, especially at the final stage.

B. Composition dependence of photodoping kinetics

Figure 5 shows the kinetics of Ag photodoping into Ge_xS_{100-x} films. A clear induction period is not observed in this experiment. However, the data of $x \geqslant 34$ show the slow rising at the early stage, being similar to the kinetic data of Ag/Ge_xSe_{100-x} samples.[5] It was judged that the phenomenon reaches the saturation level, when the optical transmission spectra deviate from λ^* (the dotted curve in Fig. 1). The saturation does not always correspond to the exhaustion of the Ag layer. For samples except $x = 30, 34,$

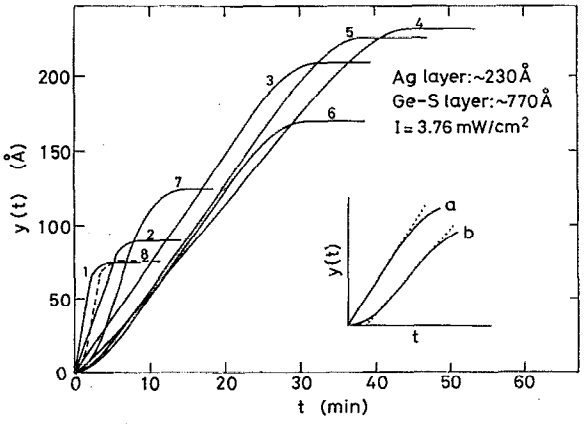

FIG. 5. Photodoping kinetics of Ag/Ge_xS_{100-x} samples ($21 < x < 45$). The curves numbered 1–8 correspond to the time courses of samples of x = 21, 24.5, 30, 34, 35, 38, 42, and 45, respectively. The parameter $y(t)$ stands for the amount of dissolved Ag (y thickness) after exposure for time t. The time course of $x = 45$ is shown by a dashed curve (8), since it probably has a relatively large experimental error. Inset shows the method evaluating IPR for the two different types of data.

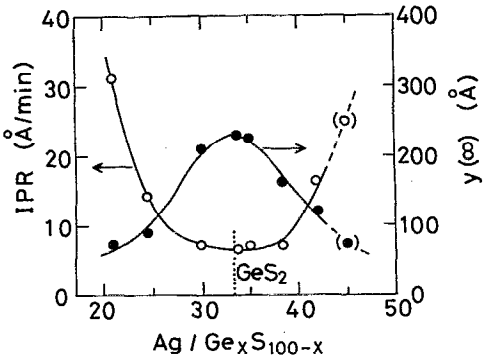

FIG. 6. Composition dependencies of IPR and total amount of photodoped Ag, $y(\infty)$, at saturation level for Ag/Ge_xS_{100-x} samples. The data of $x=45$ in parentheses probably involve a relatively large experimental error.

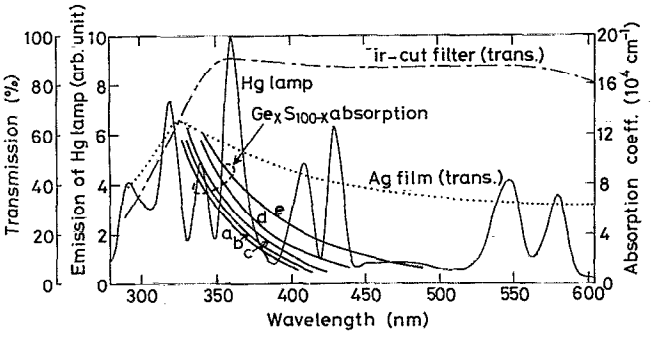

FIG. 7. Emission spectrum of ultrahigh-pressure Hg lamp, transmission spectra of ir-cut filter and Ag film (230 Å thick), and absorption coefficients of Ge_xS_{100-x} films as functions of wavelength. The curves from (a) to (e) correspond to the absorption coefficients of the samples of $x=21$, 24.5, 30, 35, and 42, respectively.

and 35, the existence of the residual Ag layer was visually observed at the saturation level. We estimated IPR and the total amount of dissolved Ag at the saturation level $y(\infty)$ from Fig. 5 and show the composition dependencies in Fig. 6.

For the composition dependence of IPR, a minimum is observed around the stoichiometric composition GeS_2. The result seems to be influenced by the emission spectrum of a light source and/or the absorption and reflection properties of Ag and chalcogenide layers. Thus, the composition dependence is necessary to be corrected for them. The photodoping is caused by the action of light absorbed in the chalcogenide layer and doped region.[7] At an early stage, the light absorbed in the chalcogenide layer contributes mainly to the photodoping.[7,20] Therefore, we corrected IPR by the total amount of the light absorbed in the Ge-S layer.

For the illumination from Ag-layer side, the incident light reaches the Ge-S layer through the Ag layer. Here, we assume that the thickness of doped region is of negligible order at the early stage. Then, the amount of light absorbed in the Ge-S layer as a function of λ, $A_{GS}(\lambda)$, is given by[21]

$$A_{GS}(\lambda)\simeq I_0(\lambda)T_{ir}(\lambda)(1-R_A)e^{-\alpha_A d_A}(1-R_{A\text{-}GS})\times[1-(1-R_{GS\text{-}G})e^{-\alpha_{GS}d_{GS}}], \quad (3)$$

where $I_0(\lambda)$ is the emission intensity of ultrahigh-pressure Hg lamp, $T_{ir}(\lambda)$ is the transmission of the ir-cut filter, R_A is the reflection coefficient at the interface between air and the Ag layer, α_A is the absorption coefficient of the Ag layer, d_A is the thickness of the Ag layer, $R_{A\text{-}GS}$ is the reflection coefficient between the Ag and Ge-S layers, $R_{GS\text{-}G}$ is the reflection coefficient between the Ge-S layer and glass substrate, α_{GS} is the absorption coefficient of the Ge-S layer, and d_{GS} is the thickness of the Ge-S layer.

Multiple reflections are neglected in Eq. (3) for simplicity.[21] It is known that if $\alpha_A d_A$ ($\alpha_{GS}d_{GS}$) >1 and/or $R_{A\text{-}GS}$ ($R_{GS\text{-}G}$) $\ll 1$, the multiple reflections can be neglected. For the Ag layer, the value of $\alpha_A d_A$ is about 2, since α_A is in the order of 10^6 cm^{-1} (300–800 nm) (Ref. 7) and d_A is about 200 Å. In contrast, $\alpha_{GS}d_{GS}$ varies from 1 to 0.1, since α_{GS} is in the order of 10^5–10^4 cm^{-1} at 350–450 nm (see Fig. 7) and d_{GS} is about 1000 Å. However, since the $R_{GS\text{-}G}$ value is as small as 0.15–0.01 in the wavelength range, Eq. (3) is considered to be a good approximation. Moreover, we approximate as $1-R_{A\text{-}GS}\simeq 1-R_A$ and $R_{GS\text{-}G}\simeq 0$ in Eq. (3). Then,

$$(1-R_A)e^{-\alpha_A d_A}(1-R_{A\text{-}GS}) \simeq (1-R_A)e^{-\alpha_A d_A}(1-R_A) = T_A(\lambda),$$

where $T_A(\lambda)$ is the transmission of the Ag layer itself. Consequently, Eq. (3) is rewritten as

$$A_{GS}(\lambda)\simeq I_0(\lambda)T_{ir}(\lambda)T_A(\lambda)(1-e^{-\alpha_{GS}d_{GS}}). \quad (4)$$

The spectra of $I_0(\lambda)$, $T_{ir}(\lambda)$, and $T_A(\lambda)$ were directly measured using the spectrophotometer. The α_{GS} value was obtained from the transmission data of the two films with different thicknesses. The respective parameters as functions of λ are shown in Fig. 7.

The total amount q of the light absorbed in the Ge-S layer is obtained as

$$q=\int A_{GS}(\lambda)d\lambda. \quad (5)$$

Equation (5) was calculated with a personal computer for the wavelength range of $\lambda_1\leqslant\lambda\leqslant\lambda_2$ corresponding to $10^3\leqslant\alpha_{GS}\leqslant 10^5$ cm^{-1}, since the light in this range effectively causes the photodoping.[10,13] The obtained q and IPR/q values are shown in Fig. 8. The composition dependence of q shows a minimum around GeS_2 and the IPR/q value decreases monotonically with increase of the Ge content.

Figure 6 also shows the composition dependence of $y(\infty)$. A maximum is observed around GeS_2. The result was checked from the amount of the residual Ag layer which was estimated from the area of the Ag(111) peak in the x-ray-diffraction pattern.

Figure 9 shows the composition dependencies of the parameters d and k. The parameter d is a coefficient con-

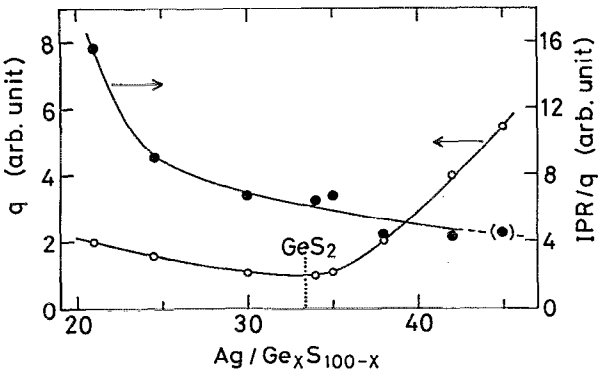

FIG. 8. Composition dependencies of q and IPR/q, where q is a parameter concerning the total amount of the light absorbed in the Ge-S layer. The q value is adjusted to unity at $x = 34$.

cerning the decrease in sample thickness by photodoping. The decrease is observed as dy, when the Ag layer of y thickness is dissolved into the Ge-S layer. The composition dependence shows a minimum around GeS_2. If the Ge-S film is well annealed before the Ag deposition onto it, the d value decreases considerably over the composition range of $21 \leqslant x \leqslant 45$. On the other hand, the parameter k is related to the change in the optical density by photodoping [Eq. (1)]. The k value was evaluated at $\lambda = 800$ nm. The composition dependence shows a maximum around GeS_2. If the Ag/Ge-S system is used as an optical recording device, the result suggests that the device with the composition around GeS_2 gives the highest contrast image, when a laser-emitting red light such as a He-Ne laser is used as a readout instrument.

IV. DISCUSSION

A. Aging effect

The aging effect has been explained by the thermal doping in the sample stored in the dark but the detail of the effect is little known. In this study, the aging effect on IPR was found to be remarkable within 5 h after the sample

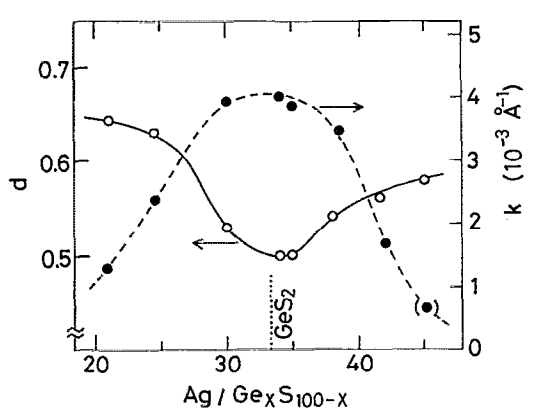

FIG. 9. Composition dependencies of d and k, where d is a parameter of decrease in sample thickness and k is a parameter of optical density change evaluated at 800 nm in wavelength. The values are normalized by the amount of photodoped Ag.

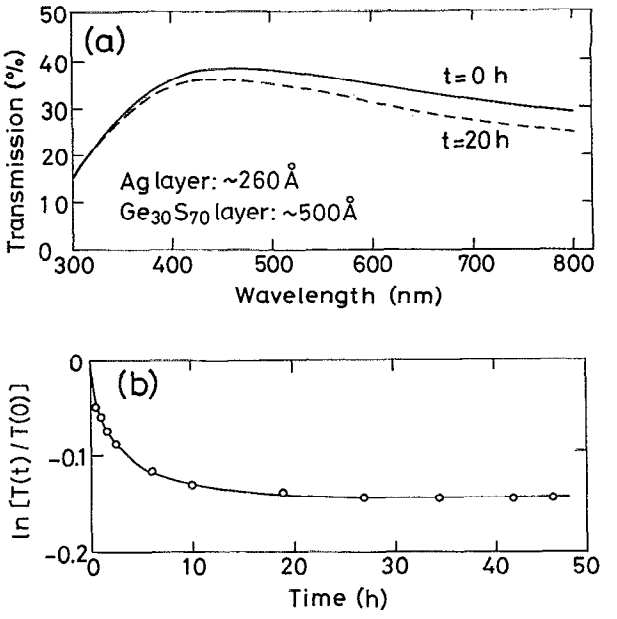

FIG. 10. (a) Change in optical transmission spectra of the $Ag/Ge_{30}S_{70}$ sample by the aging effect. (b) Time course of optical density change by aging, $\ln[T(t)/T(0)]$, at 800 nm in wavelength, where $T(t)$ is the transmission after aging time t. The data were obtained using a $Ag/Ge_{30}S_{70}$ sample aged in air (1 atm) at 16±2 °C in the dark.

preparation (Fig. 4). Since the rate of the thermal doping is considerably low at room temperature,[9] the result seems to be associated with some structural relaxation in the Ag layer and/or chalcogenide layer.

In addition to IPR, the aging effect was also found on the optical transmission spectrum of a $Ag/Ge_{30}S_{70}$ sample itself. Figure 10(a) shows the change in the spectrum of a $Ag/Ge_{30}S_{70}$ sample caused by the aging effect. The decrease of transmission is considerable at the longer-wavelength region. Figure 10(b) shows the change in the optical density evaluated at 800 nm as a function of aging time. The time course indicates that the aging effect is remarkable within 20 h after the sample preparation. The result cannot be explained by the thermal doping, since it should cause the increase of the transmission at the longer wavelength as well as the photodoping. Thus, the aging effects on the Ag and $Ge_{30}S_{70}$ films were examined separately.

As shown in Figs. 11(a) and 11(b), the aging effect was observed in both spectra. The Ag film shows the decrease in the transmission at the longer wavelength, whereas the $Ge_{30}S_{70}$ film shows slightly a blue shift of the transmission edge (thermally induced bleaching[22]). From these results, it follows that the aging effect of the photodoping sample is attributed to that of the Ag layer on the chalcogenide film. A similar result was observed for the Ag film on the glass substrate stored in a vacuum of $\sim 10^{-6}$ Torr, suggesting that a gas chemisorption such as H_2S gas ($2Ag + H_2S \rightarrow Ag_2S + H_2$) (Ref. 23) scarcely contributes to the aging effect. The thermal relaxation of the Ag film structure,[24,25] such as the homogenization of an islandlike structure, can be expected, since the decrease of transmission occurs uniformly in the range of 500–800 nm.

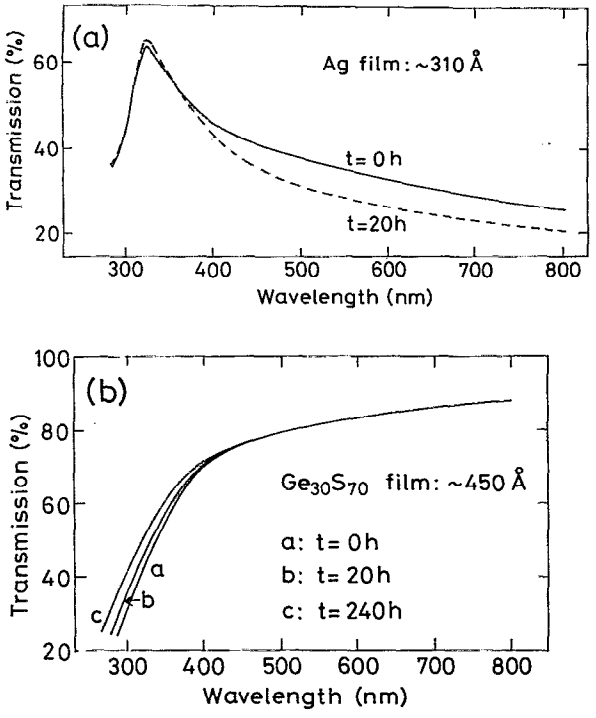

FIG. 11. Effect of aging on optical transmission spectra of (a) Ag and (b) $Ge_{30}S_{70}$ films on glass substrates. The respective samples were aged in air (1 atm) at 16±2 °C in the dark.

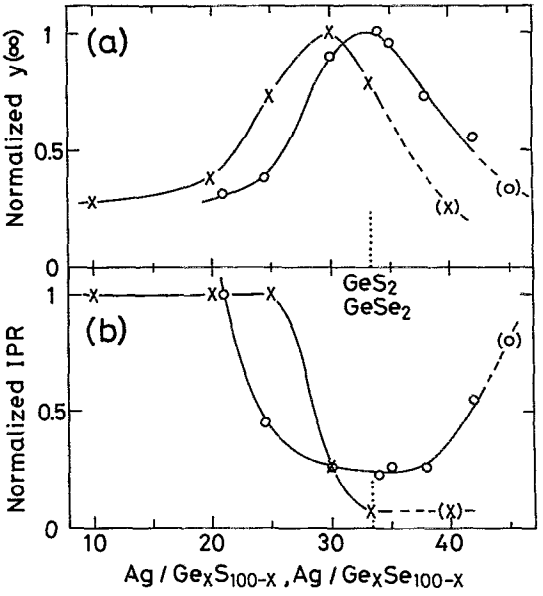

FIG. 12. Comparison of composition dependencies of (○) Ag/Ge-S and (×) Ag/Ge-Se systems for (a) $y(\infty)$ and (b) IPR. The curves are normalized by putting the maximum value to unity.

B. Reciprocity law

If the reciprocity law concerning the illumination power holds in the photodoping kinetics, the phenomenon can be purely regarded as the photoprocess and the thermal process is hidden in the background of the phenomenon. The difference in the activation energy of the Ag doping rate between photodoping (0.18 eV) and thermal doping (1.6 eV) (Ref. 11) also suggests that the photodoping phenomenon is governed by the photoprocess. Our result of the reciprocity law (Fig. 3) and the large difference in the activation energies support the idea recently proposed by Wagner and co-workers[2,3] for the photodoping mechanism.

The kinetics after the acceleration period with the fast dissolution rate did not exactly satisfy the relation of the reciprocity law, i.e., the rate normalized by light intensity was relatively greater at low-power illumination than at high power. The result suggests that the effect of the thermal process appears slightly in the phenomenon at the decay period toward the saturation level.

C. Composition dependence

Recently, Kluge *et al.*[5] reported the photodoping kinetics of Ag/Ge_xSe_{100-x} ($10 \leqslant x \leqslant 40$) samples. Although their experimental procedures are different from ours, the kinetic data can be qualitatively compared with our results, since the sample configuration and illumination system are the same as those in this study.

Figure 12(a) shows the comparison of the normalized $y(\infty)$ of Ag/Ge-S and Ag/Ge-Se systems. The respective data are taken from Fig. 6 in this paper and Fig. 3 in Ref. 5. Since the data of $x = 40$ for the Ag/Ge-Se system are ambiguous, they are shown in parentheses, as is $x = 45$ of the Ag/Ge-S system. Both composition dependencies are similar to each other and show a maximum around the stoichiometric composition (GeS_2 and $GeSe_2$). However, this result is different from the data reported for the Ag/As-S system (minimum around AsS_2,[14] almost constant[3]).

The $y(\infty)$ value is closely related to the solubility of Ag in chalcogenide film, i.e., the thermodynamic stability of Ag-containing amorphous phase (amorphous-forming ability). In connection with this, the composition dependence is qualitatively explained by the glass-forming ability of the Ag-Ge-S system: The glass-forming region is limited to less than 35 at. % for Ag content in a triangle formed by the $Ag\text{-}Ge_{30}S_{70}$ and $Ag\text{-}Ge_{45}S_{55}$ lines.[26,27] If the Ag-Ge-S phase is prepared by an evaporation method, however, the amorphous region extends considerably, as revealed by the data of the $(Ge_{0.3}S_{0.7})_{100-x}Ag_x$ system (amorphous region: $0 \leqslant x \leqslant 67$).[28] The fact supports that the photodoping can be observed in the film sample, even if the composition fairly deviates from the glass-forming region.

The raw data of IPR before the correction (Fig. 6) can be compared with the data of Kluge *et al.*,[5] as shown in Fig. 12(b). Although the comparison of the data is limited to the range of $20 \leqslant x \leqslant 34$, it can be said that both curves are similar to each other and the IPR decreases with an increase in the Ge content toward GeS_2 and $GeSe_2$ compositions. In this study, moreover, the IPR of the Ag/Ge-S system was corrected by the parameter q concerning the total photon flux absorbed in the Ge-S layer. The IPR/q value in the range of $x \leqslant 25$ increases considerably with increase of the S content (Fig. 8). The result is related to

the fact that the free sulfur (which easily reacts with Ag) is present in the Ge-S layer of $x \leqslant 25$.[29,30] Since the reaction between the free sulfur and Ag proceeds quickly,[2] the slow rising at the early stage is hardly observed in the S-rich region (Fig. 5).

The composition dependence of IPR for the Ag/Ge-S(Se) system is different from that for the Ag/As-S system (increases up to $As_{30}S_{70}$ and decreases with increasing S content[2,14]). The result for the Ag/As-S system was explained by Wagner and co-workers:[3] the maximum rate occurs near the composition with the lowest compactness of structure (the greatest molar volume) in view of the diffusion of the Ag ion. In the case of the Ge-S system, the molar volume of Ge_xS_{100-x} bulk glass ($25 < x < 44$) increases with increase of the S content except around GeS_2.[31] Therefore, the monotonic increase of IPR for the Ag/Ge-S(Se) system is qualitatively explained by the same idea.

However, the details cannot be fully explained by the structure of Ge-S bulk glass and the glass-forming ability of Ag-Ge-S bulk glass, though such explanations are successful in the Ag/As-S system.[2,3] Further, the difference in the glass-forming regions of the Ag-Ge-S (Refs. 26 and 27) and Ag-Ge-Se (Ref. 32) systems does not lead to the similarity of the composition dependencies. Strictly speaking, the photodoping phenomena of Ag/Ge-S(Se) systems must be discussed on the basis of the film properties of Ge-S(Se) systems and the amorphous-forming ability for the film samples of Ag-Ge-S(Se) systems. Actually, the physical properties and the structure of Ge-S film are considerably different from those of bulk glass with the same composition,[33] and the difference seems to be more significant than that of the As-S system. Preparations of Ag-Ge-S(Se) film samples by evaporating bulk glass and metallic Ag simultaneously using two W baskets are now in progress to elucidate the amorphous-forming regions of the film samples.

V. CONCLUSION

The composition dependence of Ag photodoping into Ge_xS_{100-x} ($21 \leqslant x \leqslant 45$) films was studied using optical transmission measurements. The kinetic data were compared with the results reported for Ag/Ge_xSe_{100-x} ($10 \leqslant x \leqslant 40$) samples. The aging effect for the photodoping sample and the reciprocity law concerning the illumination power were also examined using a $Ag/Ge_{30}S_{70}$ sample. In summary, the results are as follows.

(i) The initial photodoping rate (IPR) increases with increasing S content. The total amount of photodoped Ag, $y(\infty)$, at the saturation level shows a maximum around the stoichiometric composition GeS_2. The composition dependencies are similar to those of the Ag/Ge-Se system but are different from those of the Ag/As-S system. They are qualitatively explained by the structure of Ge-S bulk glass and the glass-forming ability of Ag-Ge-S bulk glass.

(ii) The decrease in the sample thickness by photodoping shows a minimum around GeS_2, whereas the change in the optical density evaluated at 800 nm in wavelength shows a maximum around GeS_2.

(iii) The aging effects at room temperature are remarkable within 5 h for IPR and 20 h for the optical transmission spectrum after the sample preparation.

(iv) It was found using the well-aged $Ag/Ge_{30}S_{70}$ sample that the reciprocity law holds between IPR and the illumination power.

ACKNOWLEDGMENTS

The authors would like to thank Professor K. Tanaka of Hokkaido University for valuable comments. This work was partially supported by a Grant-in-Aid for Scientific Research from the Ministry of Education, Science and Culture. T.K. gratefully acknowledges financial support from the Research Foundation for the Electrotechnology of Chubu.

[1] K. Saito, Y. Utsugi, and A. Yoshikawa, J. Appl. Phys. **63**, 565 (1988).
[2] T. Wagner and M. Frumar, J. Non-Cryst. Solids **116**, 269 (1990).
[3] T. Wagner, M. Frumar, and V. Suskova, J. Non-Cryst. Solids **128**, 197 (1991).
[4] J. Calas, R. El Ghrandi, and G. Galibert, J. Phys. (Paris) **51**, 2449 (1990).
[5] G. Kluge, A. Thomas, R. Klabes, R. Grotzschel, and P. Suptitz, J. Non-Cryst. Solids **124**, 186 (1990).
[6] T. Kawaguchi and K. Masui, Jpn. J. Appl. Phys. **26**, 15 (1987).
[7] T. Kawaguchi, S. Maruno, and K. Masui, J. Non-Cryst. Solids **95&96**, 777 (1987).
[8] A. Doi, H. Sakai, M. Yamamoto, T. Kawaguchi, and S. Maruno, Jpn. J. Appl. Phys. **29**, 313 (1990).
[9] J. M. Oldale and S. R. Elliott, J. Non-Cryst. Solids **128**, 255 (1991).
[10] D. Goldshmidt and P. S. Rudman, J. Non-Cryst. Solids **22**, 229 (1976).
[11] J. Plocharski, J. Przyluski, and M. Teodorczyk, J. Non-Cryst. Solids **93**, 303 (1987).
[12] J. H. S. Rennie and S. R. Elliott, J. Non-Cryst. Solids **77&78**, 1160 (1985).
[13] T. Wagner, M. Frumar, and L. Benes, J. Non-Cryst. Solids **90**, 517 (1987).
[14] P. J. S. Ewen, A. Zakery, A. P. Firth, and A. E. Owen, Philos. Mag. B **57**, 1 (1988).
[15] K. Konan, R. R. Elghrandi, G. Galibert, and J. Calas, J. Non-Cryst. Solids **116**, 63 (1990).
[16] K. D. Kolwicz and M. S. Chang, J. Electrochem. Soc. **127**, 135 (1980).
[17] W. Lenng, N. W. Cheung, and A. R. Neureuther, Appl. Phys. Lett. **46**, 481 (1985).
[18] Y. Yamamoto, T. Itoh, T. Hirose, and H. Hirose, J. Appl. Phys. **47**, 3603 (1976).
[19] J. H. S. Rennie, S. R. Elliott, and C. Jeynes, Appl. Phys. Lett. **48**, 1430 (1986).
[20] M. Janai, Proc. Electrochem. Soc. **82-9**, 239 (1982).
[21] M. Janai, Phys. Rev. Lett. **47**, 726 (1981).
[22] T. Kawaguchi and S. Maruno, Jpn. J. Appl. Phys. **27**, 2199 (1988).
[23] M. A. Butler and A. J. Ricco, Appl. Phys. Lett. **53**, 1471 (1988).
[24] R. B. Belser, J. Appl. Phys. **28**, 109 (1957).
[25] H. Jaeger, P. D. Mercer, and R. G. Sherwood, Surf. Sci. **13**, 349 (1969).
[26] Y. Kawamoto, N. Nagura, and S. Tsuchihashi, J. Am. Ceram. Soc. **56**, 289 (1973).
[27] A. Feltz and C. Thieme, Z. Chem. **14**, 32 (1974).
[28] S. Maruno, J. Non-Cryst. Solids **59&60**, 933 (1983).
[29] Y. Kawamoto and S. Tsuchihashi, J. Am. Ceram. Soc. **54**, 131 (1971).
[30] G. Lucovsky, F. L. Galeener, R. C. Keezer, R. H. Geils, and H. A. Six, Phys. Rev. B **10**, 5134 (1974).
[31] E. A. Zhilinskaya, V. N. Lazukin, N. Kh. Valeev, and A. K. Oblasov, J. Non-Cryst. Solids **124**, 48 (1990).
[32] J. D. Westwood, P. Georgopoulos, and D. H. Whitmore, J. Non-Cryst. Solids **107**, 88 (1988).
[33] K. Tanaka, Y. Kasanuki, and A. Odajima, Thin Solid Films **117**, 251 (1984).